ISSN: 1410-8917
Jurnal Kimia Sains & Aplikasi
e-ISSN: 2597-9914

Jurnal Kimia Sains dan Aplikasi 27 (9) (2024): 426-435

Jurnal Kimia Sains dan Aplikasi
Journal of Scientific and Applied Chemistry

Journal homepage: http://ejournal.undip.ac.id/index.php/ksa

Design and In-silico Study of ^{131}Iodium Radiolabeled of Thiourea Derivatives for Breast Cancer Treatment

Miqdad Nurabdullah Al Anshari [1], Anindita Tri Kusuma Pratita [1], Ruswanto Ruswanto [1,*]

[1] Department of Pharmacy, Faculty of Pharmacy, Bakti Tunas Husada University, Tasikmalaya, Indonesia

* Corresponding author: ruswanto@universitas-bth.ac.id

https://doi.org/10.14710/jksa.27.9.426-435

Article Info

Article history:

Received: 02nd March 2024
Revised: 17th August 2024
Accepted: 04th September 2024
Online: 30th September 2024

Keywords:
Breast cancer; in silico; radiopharmaceutical

Abstract

Breast cancer is a serious challenge in both developed and developing countries, with current therapies still limited and potentially producing adverse side effects. To optimize breast cancer drug development, this study adopted an in-silico design approach. The aim is to develop radiopharmaceutical drugs with minimal side effects. Methods involved molecular docking analysis, molecular dynamics, drug scan, and pharmacokinetic profile prediction of the original ligan as well as the radioligand. Results showed that the radioligand had better binding energy and inhibition constant than tamoxifen as a comparator drug which is -11.31 kcal/mol and 0.00511 µM. Molecular dynamics analysis revealed that the radioligand compound exhibits comparable RMSD, RMSF, and stability metrics to the native ligand at the GRPR receptor with average RMSD and RMSF of 5.263 Å and 2.285 Å, respectively. By considering the results of these various methods, the radioligand compound shows potential as an effective radiopharmaceutical drug in breast cancer therapy.

1. Introduction

Cancer, a prevalent non-communicable disease globally, continues to escalate in both occurrence and fatality annually. According to GLOBOCAN data from 2018, there were 18.1 million new cases and 9.6 million deaths worldwide. Projections from WHO suggest these numbers could soar to 26 million cases and 17 million deaths by 2030. Of particular concern is breast cancer, now outranking lung cancer as the most common cancer among women worldwide since 2020. In Indonesia, breast cancer affects 18 out of 100,000 women, indicating a significant incidence rate [1, 2].

Current cancer therapeutic approaches include small-molecule chemotherapy, surgery, radiation therapy, and radiopharmaceutical therapy. Radiopharmaceutical therapy stands out as a promising option with a lower risk of side effects. RPT uses radionuclides to deliver radiation systemically or locally to tumor-related targets [1, 3, 4, 5, 6]. Radiopharmaceuticals, radioactive compounds in nuclear medicine, are used mostly for diagnosis (95%) and a small percentage for therapy (5%). Radiopharmaceuticals employ pharmaceutical elements to guide radioactivity to specific areas within the body, facilitating detailed imaging of organs and tissues for disease diagnosis at a molecular scale [7, 8]. Radiopharmaceutical therapy typically comprises three key elements: a vector molecule, a radionuclide used for diagnosis or treatment, and the connection between them. Radionuclides emit radiation, targeting biomolecules in tissues or cells through vector molecules [8].

The development of molecular vectors incorporating thiourea and polyamine compounds is a key component in providing specific and selective anticancer effects. Thiourea compounds are known to have high effectiveness as anti-cancer agents, and many studies have focused on developing thiourea-based compounds as cancer drugs. Different thiourea-containing compounds have undergone design and testing across a range of cancer cell types, including breast (MCF-7, T-47D, MDA-MB-453), colorectal (HCT-116, LoVo), and lung cancer cells (A-549, NCI-H480), among others. Meanwhile, the main mechanism associated with the anti-cancer effects of polyamines involves the inhibition of polyamines biosynthesis, which inhibits cancer cell proliferation. Thiourea compounds, for example, have

shown the ability to inhibit polyamine biosynthesis, creating potential as anti-cancer agents; the combination of the two groups can have a synergistic effect. Vector molecules must maintain target specificity and be able to deliver radionuclides with precision to cancer cells [9, 10, 11].

Studies conducted by Arafa *et al.* [12] showed that naphthoyl thiourea-derived compounds have a superior ability to bind metal ions due to the presence of two chelating groups, namely C=S and C=O, making them potential for radiolabelling with I-131. In vitro studies on MCF-7, A549, and HCT116 cancer cells showed that these compounds not only have good anticancer activity but also show lower toxicity effects, indicating their potential use as vectors in radiopharmaceutical therapy with high efficacy and tolerability.

Drug discovery and development is a process that consumes significant time and resources. To streamline these steps, computer-aided or in silico design is used to accelerate identification, optimize absorption, distribution, metabolism, excretion and toxicity (ADMET) profiles, and avoid safety concerns. In silico modeling not only reduces the time and resources required for biological synthesis and testing but also enriches molecular groups with desirable properties and eliminates undesirable ones [7].

Therefore, it is necessary to conduct research related to the in-silico design of radiopharmaceutical compounds to improve cost and time efficiency, enable understanding of the compound's mechanism of action, and optimize molecular design. In addition, in-silico can predict toxicity and side effects before experimental trials, ensure proper target selection, and support multidisciplinary approaches. Utilizing this technology is expected to improve treatment effectiveness and reduce unwanted side effects in breast cancer patients.

2. Experimental

The study employed in silico experiments to assess the drug-like properties of a naphthoyl thiourea-derived compound and its radiolabeled variants. Various analyses, including molecular docking, dynamics, and pharmacokinetic predictions, were conducted to evaluate their potential as inhibitors of the gastrin-releasing peptide receptor.

2.1. Materials and Tools

The materials used in this study were 1-(3-{[(naphthalene-2-ylformamido) methanethioyl] amino} propyl)-3-(naphthalene-2-carbonyl) thiourea ligand, N-[(Z)-[(^{131}I) iodosulfanyl] [(3-{[(naphthalen-2-ylformamido) methanethioyl] amino} propyl) imino] methyl] naphthalene-2-carboxamide complex, the comparator compounds of anti-cancer drug tamoxifen and Gastrin-Releasing Peptide Receptor (GRPR) (PDB ID 7W41).

The tools used in this research included several software and hardware. Various software used were AutodockTools 1.5.7, MarvinSketch 23.13, Discovery Studio 21.1, Desmond software for academic license (D.E. Shaw Research, New York), Molegro, and web-based programs including Protein Data Bank, PubChem, pkCSM. Meanwhile, the hardware used in this research was a portable computer with specifications AMD Ryzen 5 5500U with Radeon Graphics @ 2.1 GHz (12 CPUs), 8 GB DDR4 RAM, and Window 11 64-Bit operating system and Intel i7 9700k GTX 1070 Ti 8GB DDR5 Ram 32GB LPX DDR4 2666MHz Linux Ubuntu OS.

2.2. Target Receptor Identification

Receptors were chosen based on specific criteria outlined in the Ramachandran Plot, ensuring disallowed regions comprised less than 0.8% when entering the receptor PDB code on http://www.ebi.ac.uk/pdbsum/ [13]. The further evaluation involved ERRAT analysis and verified 3D checks via the website https://saves.mbi.ucla.edu/. The Ramachandran plot revealed 90.9% ERRAT values within the targeted region, indicating strong structural stability and reliability [14, 15]. VERIFY 3D was employed to assess the compatibility between a 3D atomic model and its amino acid sequence, with a minimum requirement of 80% of amino acids scoring ≥ 0.2 in the 3D/1D profile being acceptable according to the Verify 3D server [16].

2.3. Ligand Preparation

The compound was drawn, followed by ligand preparation in two steps. Initially, the ligand was purified in a 2D format, protonated at a pH matching blood pH (7.4), and saved in .mrv format. Subsequently, its energy was minimized through ligand conformation and saved in .pdb format. These processes were conducted using MarvinSketch version 23.13 software by Chemaxon [13].

2.4. Docking Validation

Validation of the method involved redocking the native ligand onto the active site of the receptor, each receptor having a grid box tailored to its ligand's size and coordinates. The effectiveness was determined by calculating the Root Mean Square Deviation (RMSD) in angstroms (Å), with a value of ≤ 2 Å considered valid. AutoDockTools v.1.5.7 was employed for this purpose [17].

2.5. Molecular Docking

AutodockTools 1.57 software facilitated molecular docking, which analyzes protein-ligand interactions. Ligands must be converted to PDBQT format before docking. The grid box aligned with previous validations. Default docking, employing 150 runs with the LGA method, was used to assess ligand interactions, focusing on binding energy [13, 18, 19, 20].

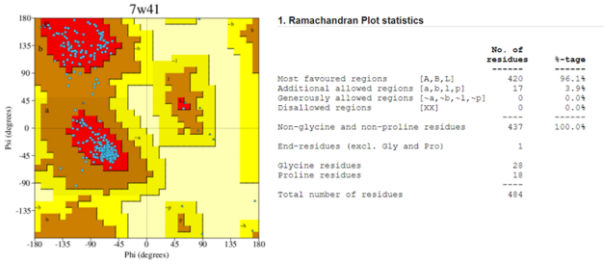

Figure 1. Ramachandran plot of 7W41

Table 1. Molecular docking validation result

Grid box dimension			Grid center			RMSD (Å)	Binding affinity (kcal/mol)	Run
X	Y	Z	X	Y	Z			
-22.555	5.292	-11.338		40		0.79	-11.47	78

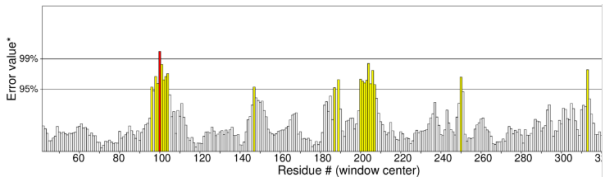

Figure 2. ERRAT value of 7W41

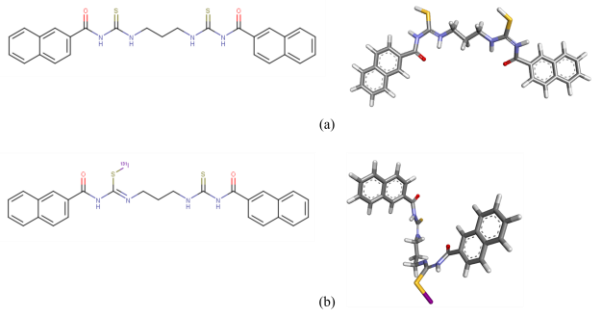

Figure 3. The 2D and 3D structures of (a) 1-(3-{[(naphthalene-2-ylformamido) methanethioyl] amino} propyl)-3-(naphthalene-2-carbonyl) thiourea and (b) N-[(Z)-[(^{131}I) iodosulfanyl] [(3- {[(naphthalene-2- ylformamido) methanethioyl] amino} propyl) imino] methyl] naphthalene-2-carboxamide

2.6. Analysis and Visualization of Docking Results

The visualization of ligand-receptor interactions in both 2D and 3D was expressed through visualization of docking results. This process identified the ligand-receptor conformation with the lowest free binding energy, generating a .pdb archive. Visualization was facilitated by Discovery Studio software [17].

2.7. Molecular Dynamics

Desmond was utilized for molecular dynamics to assess the test compound's stability with the receptor. The simulation included TIP3P water modeling and 0.15 M NaCl to mimic physiological ionic conditions. Energy minimization lasted for 100 ps, followed by a 100 ns molecular dynamics run at 300 K and 1.01325 bar pressure in an orthorhombic box with 10 Å × 10 Å × 10 Å dimensions and an NPT ensemble [21].

2.8. Ligand-based Drug Similarity Screening (Drug Scan)

Drug scan analysis was employed to assess candidate compounds after the docking and molecular dynamics phases to gauge their suitability as potential oral medications for humans, following Lipinski's Rule of Five. This rule, outlined at http://www.scfbio-iitd.res.in/software/drugdesign/lipinski.jsp, defined criteria such as molecular mass below 500 daltons, LogP under 5, molar refraction ranging from 40 to 130, fewer than 5 hydrogen bond donors, and fewer than 10 hydrogen bond acceptors. Compounds exhibiting lower free energy than the native ligand underwent this evaluation, ensuring alignment with Lipinski's criteria for drug categorization [22, 23].

2.9. Prediction of Pharmacokinetic and Toxicity Profile

The pkCSM website tool was utilized to forecast the pharmacokinetic attributes, including absorption, distribution, metabolism, and excretion, alongside toxicity, of the test compounds. Compound data entered for prediction was converted into SMILES format [24].

3. Results and Discussion

3.1. Target Receptor Identification

Evaluation of protein quality involves receptor identification, employing criteria such as Ramachandran plot parameters from http://www.ebi.ac.uk/pdbsum/, profile checking, ERRAT analysis, and VERIFY 3D via https://saves.mbi.ucla.edu/ [13, 14]. The receptor under examination, Gastrin-Releasing Peptide Receptor (GRPR) with PDB ID: 7W41, is utilized. Ramachandran plots, showcasing phi-psi dihedral angles for all residues except chain ends, illustrate protein stereochemistry distribution in two dimensions. These plots delineate four regions: most favored, additional allowed, broadly allowed, and prohibited. Ideally, a high-quality protein structure would exhibit over 90% of its residues within the most favored region [25]. The Ramachandran plot analysis confirms the receptor's stable and high-quality structure, with 96.1% adherence to quadrant I and no violations in quadrant IV (Figure 1). Thus, it is suitable for further stages of study.

ERRAT, a method for pinpointing faults in protein structures due to atom distribution inaccuracies, evaluates quality based on the proportion of proteins failing the 95% rejection benchmark. Lower resolution structures generally score near 91%. With an ERRAT value of 92.842%, it is evident that the 7W41 receptor exhibits low-resolution (Figure 2) [26].

3.2. Receptor and Ligand Preparation

To prepare the ligand, it is protonated and adjusted to match the blood pH (7.4) and conformation. This ensures the ligand is in its most stable energy position to interact with the receptor's active site effectively. MMFF94 works well in optimizing geometry, bond length, and angle and includes electrostatic effects and hydrogen bonding [27]. Out of ten conformation trials, the one with the least energy was chosen for the subsequent step, as depicted in Figure 3. Simultaneously, receptor preparation involves eliminating water molecules to prevent interference with ligand-receptor interactions [17].

Table 2. Docking results against GRPR receptor

Compound	ΔG (kcal/mol)	Ki (μM)	Residue interaction	
			Hydrogen bonds	van der Waals
Native ligand	-12.16	0.00121	SER A:179, **GLU A:175**, GLN A:120, TYR A:468, TYR A:199, PRO A:200	**TRP A:106**, **SER A:214**, LEU A:121, **ILE A:116**, VAL A:96, PHE A:178, VAL A:124, **ASN A:464**, CYS A:93, PRO A:207, HIS A:206
Original ligand	-10.26	0.02994	**GLU A:175**	ARG A:100, ARG A:471, LEU A:121, **HIS A:210**, GLN A:120, **ASN A:464**, **TRP A:106**, **ILE A:116**, **SER A:179**, VYS A:113
Radioligand	-11.31	0.00511	**GLU A:175**, TYR A:199, TYR A:468	PRO A:200, PHE A:178, **HIS A:210**, **SER A:179**, GLN A:120, ILE A:467, **SER A:214**, VAL A:124, PHE A:218, TRP A:461, **ASN A:464**
Tamoxifen	-7.53	3.02	-	LEU A:89, TRP A:461, **ASN A:464**, **SER A:214**, ARG A:492, GLN A:120, **HIS A:210**, GLU A:175, **SER A:179**, **ILE A:116**, PRO A:198, CYS A:113, **TRP A:106**, CYS A:196

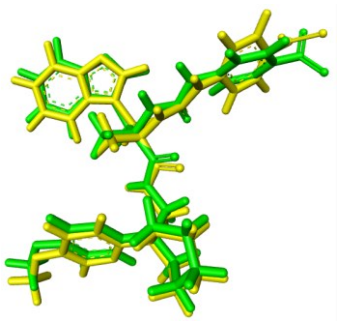

Figure 4. Results of native ligand stacks before redocking (green) and after redocking (yellow)

3.3. Docking Validation

Confirmation of the method's validity was achieved by reattaching a native ligand to the active site of a previously dissociated receptor in 150 different conformations. (8B8) was reattached to gastrin-releasing peptide receptor (7W41). Figure 4 displays an overlay image comparing the crystallographic structure with the re-docking outcome. Additional specifics, such as grid box size, coordinates, and re-bonding result values, are outlined in Table 1.

Receptor validation relies on comparing changes in ligand distance and conformation before and after re-pairing. If the resulting RMSD value is < 2 Å, the re-docking is deemed valid for tethering studies [17].

3.4. Molecular Docking

Molecular docking compared the test ligand, N-[(Z)-[(131I) iodosulfanyl] [(3-{[(naphthalen-2-ylformamido) methanethioyl] amino} propyl) imino] methyl] naphthalene-2- carboxamide, with the original ligand 1-(3-{[(naphthalene-2-ylformamido) methanethioyl] amino} propyl) -3-(naphthalene-2-carbonyl) thiourea, tamoxifen, and the native ligand of the GRPR receptor ((2S)-3-(1H-indol-3-yl)-N-[[1-(5-methoxypyridine-2-yl)cyclohexyl]methyl]-2-methyl-2-[(4-nitrophenyl)carbamoylamino]propanamide) across 150 conformations.

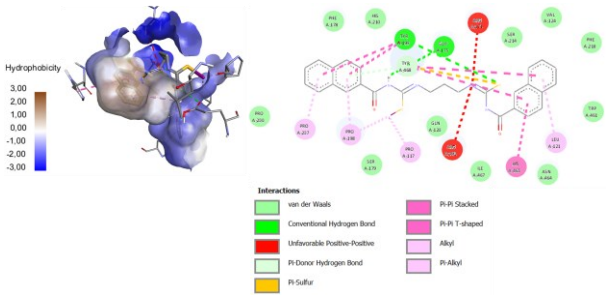

Figure 5. The 3D and 2D visualization of GRPR receptor of radioligand

The ΔG, measured in kcal/mol, indicates the equilibrium and stability of the protein-ligand complex. Conversely, the inhibition constant reflects the drug's potency in inhibiting receptor activity. A lower inhibition constant signifies stronger inhibition, indicating higher effectiveness in blocking receptor function [28]. Table 2 shows that the radioligand's ΔG value is not smaller than its native ligand but smaller than the comparator, namely its original ligand and breast cancer drug (Tamoxifen). Generally, the binding affinity obtained has a negative value, indicating that the ligand and receptor interaction occurs naturally. Observing the relationship between the ligand and the amino acid residues can be done through Discovery Studio software by using the .pdb files of the best docking results previously simulated. Some of the interactions that can be observed include hydrogen bonds and hydrophobic bonds.

The radioligand compound visualized the interaction of ligand and amino acid residues in 3D and 2D, shown in Figure 5. Based on the lowest binding affinity and inhibition constant values, 8B8 (native ligand) has six hydrogen bonds (SER A:179, GLU A:175, GLN A:120, TYR A:468, TYR A: 199, and PRO A:200) and eleven van der Waals bonds (TRP A:106, SER A:214, LEU A:121, ILE A:116, VAL A:96, PHE A:178, VAL A:124, ASN A:464, CYS A:93, PRO A:207, and HIS A:206). Hydrogen bonding with the GLU A:175 residue is present in 3 of the 4 compounds in sequence. This residue may play an essential role in the stability of ligand interactions with GRPR receptors.

Table 3. The RMSD and RMSF results of molecular dynamics simulation

Compound	RMSD			RMSF		
	Average	Minimum	Maximum	Average	Minimum	Maximum
Native ligand	4.274	1.67	7.418	2.843	0.906	8.044
Original ligand	6.377	1.521	9.947	3.214	1.198	8.56
Radioligand	5.263	2.05	6.695	2.285	0.838	5.801
Tamoxifen	6.289	2.211	8.428	3.864	1.208	8.682

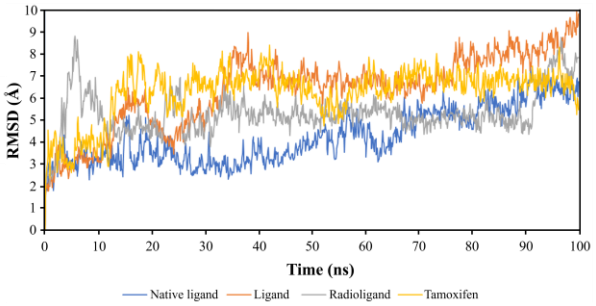

Figure 6. RMSD plot of ligand complex-GRPR

In addition to the van der Waals bond, residues TRP A:106, SER A:214, ILE A:116, ASN A:464, HIS A:210, and SER A:179 are present in 3 of the 4 compounds. While the tamoxifen compound does not form hydrogen bonds, this is because the tamoxifen compound does not have a hydrogen bond donor and only has two hydrogen bond acceptors. Hydrogen bonds are considered a type of bond that is favored in the interaction between ligands and receptors because they can affect the physicochemical properties and biological activity of the compound. The ability of a drug to dissolve in the cell membrane can be understood through hydrophobic bonds that are expected to bind to the receptor effectively. Thus, hydrogen bonding plays a vital role in determining the solubility of drugs and their interaction with cell receptors [29].

3.5. Molecular Dynamics

Molecular dynamics employs computer simulations to study how atoms and molecules interact over time, analyzing their movements and chemical behaviors. It aims to forecast atomic behavior and investigate molecular properties under diverse conditions by replicating cellular environments, applying physical forces based on physics and thermodynamics laws, and leveraging intensive computing for temporal considerations [26]. Molecular dynamics was performed on the test ligand, N-[(Z)-[(^{131}I) iodosulfanyl] [(3-{[(naphthalene-2-ylformamido) methanethioyl] amino} propyl) imino] methyl] naphthalen-2-carboxamide against GRPR receptors with the comparator being its native ligand 1-(3-{[(naphthalene-2-ylformamido) methanethioyl] amino} propyl) -3-(naphthalene-2-carbonyl) thiourea, the breast cancer drug tamoxifen as well as the GRPR receptor's native ligand ((2S)-3-(1H-indol-3-yl)-N-[[1-(5-methoxypyridine-2-yl) cyclohexyl] methyl] -2-methyl-2-[(4-nitrophenyl) carbamoylamino] propanamide).

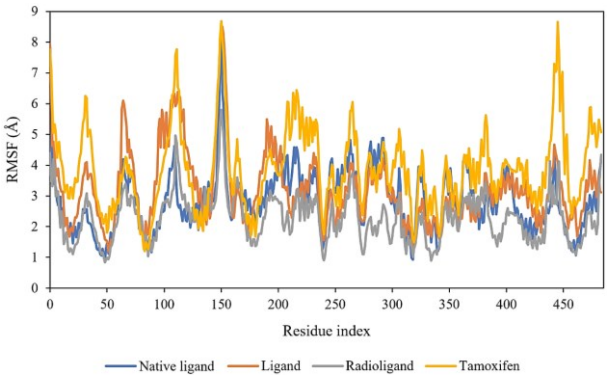

Figure 7. The RMSF plot of ligand complex-GRPR

Figure 6 illustrates the stability of various ligand-GRPR complexes during a 100 ns molecular dynamic simulation. Each ligand undergoes initial fluctuations, followed by periods of stability and subsequent fluctuations. The native ligand complex maintains stability from 3 ns to 15 ns but fluctuates afterward. The original ligand complex stabilizes from 3 ns to 10 ns, fluctuates until 55 ns, stabilizes again until 75 ns, then fluctuates. The radioligand complex stabilizes from 3 ns to 15 ns, experiences fluctuations, then stabilizes from 25 ns to 100 ns with minor fluctuations. The tamoxifen complex remains stable from 45 ns to 100 ns, with intermittent fluctuations.

Table 3 displays the interactions of different ligands, showing the mean RMSD values. The native ligand complex has the lowest RMSD (4.274 Å), followed by the radioligand complex (5.263 Å), tamoxifen complex (6.289 Å), and the original ligand complex (6.377 Å). This indicates that the radioligand complex performs better than Tamoxifen but not as well as the native ligand. Additionally, Figure 7 presents residue flexibility analysis based on the RMSF value of each test ligand.

The RMSF plot assesses interaction stability in the ligand-GRPR complex. In Figure 7, RMSF values for the native ligand, ligand, radioligand, and tamoxifen complexes are compared. Fluctuations occur in similar regions, with the radioligand complex exhibiting the least fluctuation. Average RMSF values for the complexes are radioligand (2.285 Å), native ligand (2.843 Å), original ligand (3.214 Å), and tamoxifen (3.864 Å). Results suggest similar residue motion patterns across all compounds, with higher flexibility at the protein's termini and lower flexibility elsewhere. This suggests that ligand binding causes little change in protein structure. Molecular dynamics simulations also uncover alterations in hydrogen and hydrophobic bonds within each ligand-GRPR complex, alongside analyses of RMSD and RMSF.

Table 4. Lipinski's Rule of Five analysis results

Compound	Parameter				
	Mass	Hydrogen bond donors	Hydrogen bond acceptors	LogP	Molar refractivity
	<500 g/mol	<5	<10	<5	40-130
1-(3-{[(naphthalene-2-ylformamido) methanethioyl] amino}propyl)-3-(naphthalene-2-carbonyl) thiourea	502	4	4	1.2757	147.090897
N-{[(^{131}I) iodosulfanyl] [(3-{[(naphthalene-2-ylformamido) methanethioyl] amino}propyl) imino] methyl}naphthalene-2-carboxamida	630	4	3	3.865699	160.669952
Tamoxifen	371	0	2	5.996100	119.581955

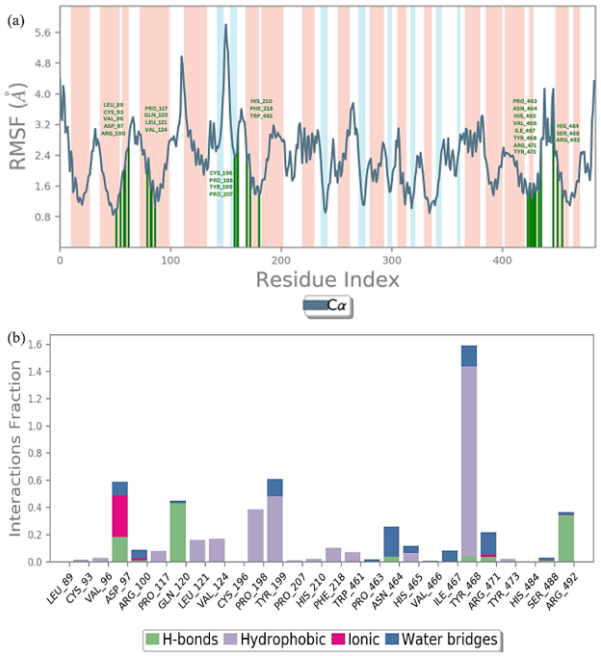

Figure 8. (a) RMSF graph of GRPR protein complex, (b) interaction of amino acid residues with radioligand

Figure 8 shows 27 residue contacts with radioligand compounds through several types of bonds, namely hydrogen bonds (ASP:97, GLN:120, ASN:464, TYR:468, ARG:471, SER:488, and ARG:492), hydrophobic (CYS:93, VAL:96, PRO:117, LEU:121, VAL:124, PRO:198, TYR:199, PRO:207, HIS:210, PHE:218, TRP:461, HIS:465, TYR:468, and TYR:473), ionic (ASP:97, ARG:100, ARGl471, SER:488, and ARG:492), and water bridges (CYS:93, ASP:97, ARG:100, GLN:120, TYR:199, PRO:463, ASN:464, HIS:465, VAL:466, ILE:467, TYR:468, ARG:471, SER:488, and ARG:492).

Six parameters of characterization (as depicted in Figure 9(a)) were examined to elucidate the stability of the radioligand illustrated in the same figure. Throughout the molecular dynamics simulation, the radioligand compound displayed consistent stability, with RMSD fluctuating between 0.7 Å and 1.6 Å. The radius of gyration (rGyr) varied from 4.15 Å to 4.65 Å, reflecting the ligand's dynamic conformational changes over time [30]. The simulation revealed fluctuations in the number of intramolecular hydrogen bonds, ranging from 0 to 3, with a predominant occurrence of 1-2 hydrogen bonds.

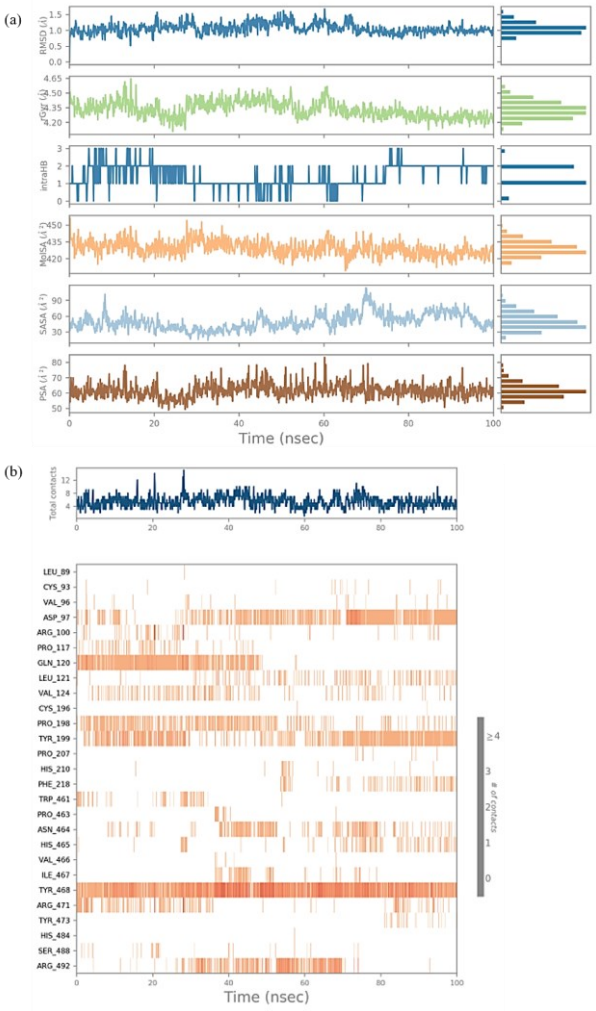

Figure 9. (a) Radioligand characterization, (b) representation of residue contacts and radioligand interactions during 100 ns molecular dynamics simulation

The MolSA values fluctuate between 415 Å^2 and 460 Å^2, stabilizing around 425 Å^2 to 430 Å^2 by the end of the simulation. Similarly, SASA fluctuates between 20 Å^2 and 100 Å^2, stabilizing between 40 Å^2 and 50 Å^2. Meanwhile, PSA fluctuates between 50 Å^2 and 80 Å^2, stabilizing around 55 Å^2 to 60 Å^2. Figure 9(b) shows the relationship between residues and ligands in each lane. Some protein residues have many specific contacts with the ligand, as indicated by the darker orange color.

Table 5. Pharmacokinetic and toxicity profile prediction

Parameter				Compound		
				1-(3-{[(naphthalene-2-ylformamido) methanethioyl] amino}propyl)-3-(naphthalene-2-carbonyl) thiourea	N-{[(^{131}I) iodosulfanyl] [(3-{[(naphthalene-2-ylformamido) methanethioyl] amino}propil) imino] methyl}naphthalene-2-carboxamida	Tamoxifen
Absorption	Caco-2		Log c/s	0.989	0.977	1.167
	Intestinal absorption		%	89.706	88.588	100
Distribution	VDss		Log L/kg	0.15	0.158	0.565
	BBB		Log BB	-0.96	-1.077	1.436
Metabolism	CYP3A4	Substrate		Yes	Yes	Yes
		Inhibitor		No	Yes	Yes
Distribution	Renal OCT2	Substrate	Yes/No	No	No	No
Toxicity	AMES toxicity			Yes	Yes	Yes
	Hepatotoxicity			Yes	No	No

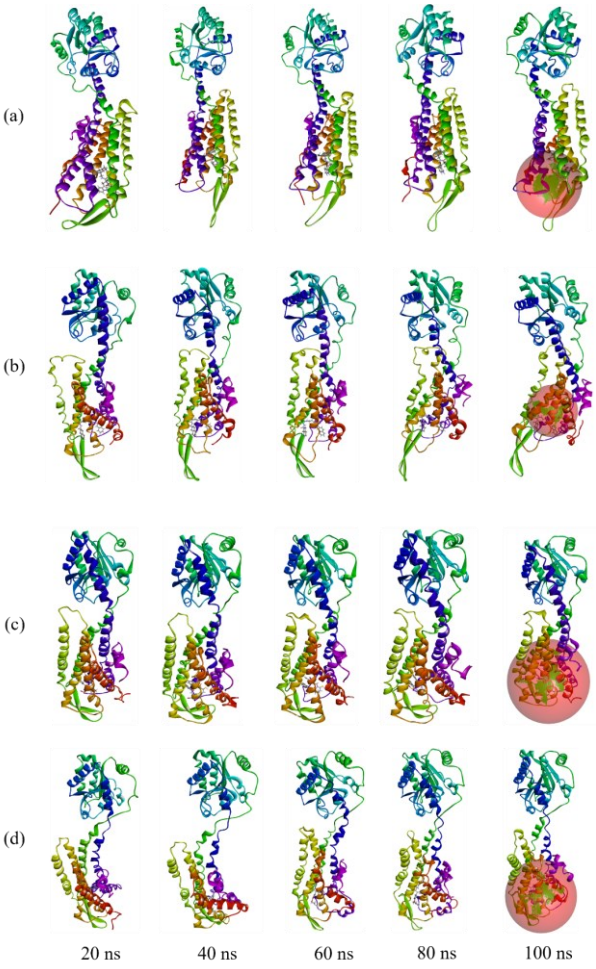

Figure 10. The conformational changes of (a) native ligand-GRPR, (b) origin ligand-GRPR, (c) radioligand-GRPR, and (d) tamoxifen-GRPR in 100 ns molecular dynamic simulation

During the 100 ns molecular dynamic simulation, changes in ligand-GRPR complexes' conformation were observed. Figure 10(a)-(d) illustrates these changes over time intervals starting from 20 to 100 ns. Across the four tested ligand complexes (Natural, Origin, Radioligand, and Tamoxifen), conformational shifts occurred consistently within the GRPR protein binding site throughout the simulation, as depicted in Figure 10.

3.6. Ligand-based Drug Similarity Screening (Drug Scan)

Lipinski's Rule of Five outlines key criteria for designing drug molecules suitable for oral administration, including lipophilicity below 5, molecular weight under 500 g/mol, fewer than 5 hydrogen bond donors, a molar refractivity (MR) between 40-130, and less than 10 hydrogen bond acceptors [31]. Lipophilicity, a fundamental property influencing a compound's pharmacokinetic profile, indicates its ability to navigate biological systems by resembling the lipophilic environment, facilitating membrane crossing and interaction with receptor-binding sites [32].

The size of a molecule influences its ability to pass through membranes in the gut and brain. Larger molecules move more slowly through lipid layers, limiting their ability to penetrate biological barriers [28]. MR is the reciprocal of a substance's molar volume and is closely linked to the total polarity of the substance. MR data reveals the electronic polarity of ions in solution, aiding in understanding molecular interactions. Optimal oral absorption and bioavailability occur when MR falls between 40 to 130. A substance within this range, along with its bonding capacity, suggests favorable intestinal absorption and oral bioavailability [33].

Lipinski's supplementary criteria stipulate that a compound should have fewer than 10 hydrogen bond acceptors and fewer than 5 hydrogen bond donors. These guidelines are crucial for understanding a compound's physicochemical characteristics, particularly its ability to form hydrogen bonds. The number of hydrogen bond donors influences a compound's biological activity, while the number of acceptors affects its permeability by interacting with solvents possessing strong hydrogen bonds. Compounds interacting with polar solvents typically have decreased permeability across lipid

bilayers. A drug's overall polarization, affected by various factors such as refractive index, pressure, and temperature, correlates with its molar refractivity. This polarization depends on molecular structure and mass, with more electrons aiding in detection. Lipinski's rule of five states that compounds are compliant if they satisfy at least two of the five criteria [28]. Thus, based on screening outcomes (Table 4), these three compounds demonstrate a favorable drug similarity profile.

3.7. Predicted Pharmacokinetic and Toxicity Profile

Pharmacokinetic and toxicity profiles are used in the research and development of new drugs to evaluate the effectiveness and potential side effects of drug candidates. This assessment relies on a number of parameters, such as Caco-2, intestinal absorption, VDss, blood-brain barrier (BBB), activity as CYP3A4 substrate and inhibitor, organic cation transporter 2 (OCT2), AMES toxicity, hepatotoxicity, and LD_{50}. Table 5 presents the results of the prediction of pharmacokinetic and toxicity profiles based on these parameters, providing an overview of the possible performance and risks associated with the test ligands.

The Caco-2 cell line, derived from colorectal adenocarcinoma epithelial cells, is commonly used as an in vitro model for studying human intestinal mucosa and predicting oral drug absorption. A drug is considered to have good absorption when its Caco-2 value exceeds 0.9. Since all tested ligands have Caco-2 values above this threshold, they can be regarded as having good permeability. In addition to the Caco-2 value, a drug's absorption capability can also be evaluated through its intestinal absorption value. This metric predicts absorption in the human small intestine, with values over 80% indicating good absorption and values below 30% indicating poor absorption. Each tested ligand has an intestinal absorption value above 80%, leading to the conclusion that they exhibit good absorption in the small intestine [24].

VDss, or volume of distribution, represents the volume needed to disperse a dose to achieve a concentration similar to blood plasma. A higher VD indicates more distribution in tissues compared to plasma, potentially leading to effects like renal failure and dehydration. Logarithmically, a low VD is indicated when log VD < -0.15, while a high VD is when log VD > 0.45. The BBB serves as protection against foreign substances in the brain. Evaluation of a drug's capability to penetrate the brain becomes a crucial parameter in efforts to reduce side effects and toxicity or improve treatment effectiveness through pharmacological intervention within the brain. In certain contexts, molecules with a logBB value > 0.3 are considered to be able to easily penetrate the BBB, while those with a logBB < -1 are considered to have a more limited penetration ability into the brain.

Based on the data in Table 5, the radioligand is categorized as having limited brain distribution, as indicated by its LogBB value of -1.077, which is below the threshold of -1. In contrast, the other compounds fall within the range that suggests varying degrees of brain penetration, from easily penetrating to less dispersed [24].

The metabolic profile of a compound can be represented through several parameters that evaluate its interaction with cytochrome enzymes. Cytochrome P450, an enzyme commonly found in the liver, plays a vital role in the detoxification of the body by oxidizing xenobiotics and converting drug compounds into inactive forms. Parameters such as CYP3A4 inhibitors are used to assess the inhibition of drug molecules against cytochrome P450. In contrast, the CYP3A4 substrate is used to determine whether or not the compound is a substrate of this cytochrome enzyme [20]. All test ligands functioned as CYP3A4 substrates, and only the original ligand did not act as a CYP3A4 substrate.

The renal transporter OCT2 plays a vital role in drug delivery and eliminating natural compounds from the body. Combining OCT2 substrates with inhibitors can lead to adverse reactions. Evaluating a drug's interaction with OCT2 not only informs about its clearance but also highlights potential contraindications [20]. The three compounds looked at did not interact with this OCT2 substrate and did not affect the clearance and disposition of the compound within the kidney.

The Ames test is a widely used method to assess the mutagenicity of compounds in bacteria. A positive test indicates that the compound is mutagenic and can cause cancer. All three compounds gave positive results. Besides the Ames test, another toxicity parameter used is liver toxicity. A significant safety issue in drug development is hepatotoxicity caused by the use of drugs. It is a major focus of attention as its impact on the liver can be harmful to health. A compound is considered hepatotoxic if it causes at least one pathological or physiological event that is closely associated with disruption of normal liver function [24]. Based on Table 5, only the original ligand gave positive results.

This research identified and characterized the radioligand compound that demonstrates superior binding affinity and stability at the GRPR receptor, as evidenced by the most favorable free energy and inhibition constant among the tested ligands. This work provides a significant advancement in the development of targeted radiopharmaceuticals, particularly in the context of breast cancer treatment. The detailed molecular dynamics analysis underscores the compound's potential as a viable candidate for drug development, with comparable RMSD, RMSF, and stability metrics to the native ligand, indicating its robustness under physiological conditions. Looking ahead, the radioligand compound's unique properties position it as a promising candidate for commercial development, offering a novel therapeutic option in the realm of precision medicine for breast cancer. Future studies could focus on further preclinical evaluations, optimization of radiolabeling techniques, and exploration of its efficacy and safety in clinical settings to fully realize its potential as a commercial radiopharmaceutical drug.

4. Conclusion

The radioligand compound demonstrated the most favorable energy with a free energy of -11.31 kcal/mol and an inhibition constant of 0.00511 µM, surpassing other tested ligands, including the original ligand and tamoxifen, as evidenced by extensive 100 ns molecular dynamics simulation. Notably, molecular dynamics analysis revealed that the radioligand compound exhibits comparable RMSD, RMSF, and stability metrics to the native ligand at the GRPR receptor. These findings suggest promising avenues for further investigation into the potential of the radioligand compound for the development of radiopharmaceutical drugs targeting breast cancer.

Acknowledgment

The authors thank the Universitas Bakti Tunas Husada for providing the research facilities.

References

[1] Mohammad Kaisarul Islam, Animesh Chandra Barman, Nazmul Qais, Anti-Cancer Constituents from Plants: Mini Review: Anti-Cancer Constituents from Plants: Mini Review, *Dhaka University Journal of Pharmaceutical Sciences*, 19, 1, (2020), 83-96 https://doi.org/10.3329/dujps.v19i1.47823

[2] Hyuna Sung, Jacques Ferlay, Rebecca L. Siegel, Mathieu Laversanne, Isabelle Soerjomataram, Ahmedin Jemal, Freddie Bray, Global Cancer Statistics 2020: GLOBOCAN Estimates of Incidence and Mortality Worldwide for 36 Cancers in 185 Countries, *CA: A Cancer Journal for Clinicians*, 71, 3, (2021), 209-249 https://doi.org/10.3322/caac.21660

[3] Martin R. Gill, Nadia Falzone, Yong Du, Katherine A. Vallis, Targeted radionuclide therapy in combined-modality regimens, *The Lancet Oncology*, 18, 7, (2017), e414-e423 https://doi.org/10.1016/S1470-2045(17)30379-0

[4] Sondang Khairani, Sesilia Andriani Keban, Meyke Afrianty, Evaluation of Drug Side Effects Chemotherapy on Quality of Life (QOL) Breast Cancer Patients at Hospital X in Jakarta, *Jurnal Ilmu Kefarmasian Indonesia*, 17, 1, (2019), 9-13 https://doi.org/10.35814/jifi.v17i1.705

[5] Ann Lin, Christopher J. Giuliano, Ann Palladino, Kristen M. John, Connor Abramowicz, Monet Lou Yuan, Erin L. Sausville, Devon A. Lukow, Luwei Liu, Alexander R. Chait, Zachary C. Galluzzo, Clara Tucker, Jason M. Sheltzer, Off-target toxicity is a common mechanism of action of cancer drugs undergoing clinical trials, *Science Translational Medicine*, 11, 509, (2019), eaaw8412 https://doi.org/10.1126/scitranslmed.aaw8412

[6] Chi Heem Wong, Kien Wei Siah, Andrew W Lo, Estimation of clinical trial success rates and related parameters, *Biostatistics*, 20, 2, (2018), 273-286 https://doi.org/10.1093/biostatistics/kxx069

[7] Demir Emine Selin, Ozgenc Emre, Ekinci Meliha, Gundogdu Evren Atlihan, Özdemir Derya İlem, Asikoglu Makbule, Computational Study of Radiopharmaceuticals, in: S. Amalia (Ed.) *Molecular Docking and Molecular Dynamics*, IntechOpen, Rijeka, 2019, https://doi.org/10.5772/intechopen.85140

[8] Koen Vermeulen, Mathilde Vandamme, Guy Bormans, Frederik Cleeren, Design and Challenges of Radiopharmaceuticals, *Seminars in Nuclear Medicine*, 49, 5, (2019), 339-356 https://doi.org/10.1053/j.semnuclmed.2019.07.001

[9] Robert A. Casero, Tracy Murray Stewart, Anthony E. Pegg, Polyamine metabolism and cancer: treatments, challenges and opportunities, *Nature Reviews Cancer*, 18, 11, (2018), 681-695 https://doi.org/10.1038/s41568-018-0050-3

[10] Elisabetta Damiani, Heather M. Wallace, Polyamines and Cancer, in: *Polyamines: Methods Protocols*, Humana Press, New York, 2018, https://doi.org/10.1007/978-1-4939-7398-9_39

[11] Wimzy Rizqy Prabhata, Fidya Aulannisa, Muhammad Arif Rizky Nur Rahman, Shyelivia Thesalonica, Review Artikel: Strategi Pengembangan Senyawa Thiourea Sebagai Agen Antikanker, *Generics: Journal of Research in Pharmacy*, 2, 2, (2022), 127 - 138 https://doi.org/10.14710/genres.v2i2.15916

[12] Wael Abdelgayed Ahmed Arafa, Amira Atef Ghoneim, Asmaa K. Mourad, *N*-Naphthoyl Thiourea Derivatives: An Efficient Ultrasonic-Assisted Synthesis, Reaction, and *In Vitro* Anticancer Evaluations, *ACS Omega*, 7, 7, (2022), 6210-6222 https://doi.org/10.1021/acsomega.1c06718

[13] Ruswanto Ruswanto, Amir M. Miftah, Daryono H. Tjahjono, Siswandono, In silico study of 1-benzoyl-3-methylthiourea derivatives activity as epidermal growth factor receptor (EGFR) tyrosine kinase inhibitor candidates, *Chemical Data Collections*, 34, (2021), 100741 https://doi.org/10.1016/j.cdc.2021.100741

[14] Richa Mardianingrum, Sri Rezeki Nur Endah, Eddy Suhardiana, Ruswanto Ruswanto, Siswandono Siswandono, Docking and molecular dynamic study of isoniazid derivatives as anti-tuberculosis drug candidate, *Chemical Data Collections*, 32, (2021), 100647 https://doi.org/10.1016/j.cdc.2021.100647

[15] Neha Srivastava, Prekshi Garg, Prachi Srivastava, Prahlad Kishore Seth, A molecular dynamics simulation study of the ACE2 receptor with screened natural inhibitors to identify novel drug candidate against COVID-19, *PeerJ*, 9, (2021), e11171 https://doi.org/10.7717/peerj.11171

[16] Rajnee Hasan, Md. Nazmul Haq Rony, Rasel Ahmed, In silico characterization and structural modeling of bacterial metalloprotease of family M4, *Journal of Genetic Engineering and Biotechnology*, 19, 1, (2021), 25 https://doi.org/10.1186/s43141-020-00105-y

[17] Ruswanto Ruswanto, Richa Mardianingrum, Arry Yanuar, Computational Studies of Thiourea Derivatives as Anticancer Candidates through Inhibition of Sirtuin-1 (SIRT1), *Jurnal Kimia Sains dan Aplikasi*, 25, 3, (2022), 87-96 https://doi.org/10.14710/jksa.25.3.87-96

[18] Muhammad Ashraf, Rafaqat Hussain, Shoaib Khan, Wajid Rehman, Yousaf Khan, Asma Sardar, Tariq Aziz, Manal M. Khowdiary, In vitro and in silico correlation of benzoxazole-based thiazolidinone hybrids derivatives: A promising acetylcholinesterase and butyrylcholinesterase inhibitors, *Journal of Molecular Structure*, 1301,

(2024), 137317
https://doi.org/10.1016/j.molstruc.2023.137317

[19] Rafaqat Hussain, Wajid Rehman, Shoaib Khan, Fadi Jaber, Fazal Rahim, Mazloom Shah, Yousaf Khan, Shahid Iqbal, Haseena Naz, Imran Khan, Mohammed Issa Alahmdi, Nasser S. Awwad, Hala A. Ibrahium, Investigation of novel bis-thiadiazole bearing schiff base derivatives as effective inhibitors of thymidine phosphorylase: Synthesis, in vitro bioactivity and molecular docking study, *Saudi Pharmaceutical Journal*, 31, 11, (2023), 101823 https://doi.org/10.1016/j.jsps.2023.101823

[20] Yousaf Khan, Shoaib Khan, Rafaqat Hussain, Aneela Maalik, Wajid Rehman, Mohamed W. Attwa, Rafia Masood, Hany W. Darwish, Hazem A. Ghabbour, The Synthesis, In Vitro Bio-Evaluation, and In Silico Molecular Docking Studies of Pyrazoline - Thiazole Hybrid Analogues as Promising Anti- α - Glucosidase and Anti-Urease Agents, *Pharmaceuticals*, 16, 12, (2023), 1650 https://doi.org/10.3390/ph16121650

[21] Sumit Kumar, Prem Prakash Sharma, Uma Shankar, Dhruv Kumar, Sanjeev K. Joshi, Lindomar Pena, Ravi Durvasula, Amit Kumar, Prakasha Kempaiah, Poonam, Brijesh Rathi, Discovery of New Hydroxyethylamine Analogs against $3CL^{pro}$ Protein Target of SARS-CoV-2: Molecular Docking, Molecular Dynamics Simulation, and Structure–Activity Relationship Studies, *Journal of Chemical Information and Modeling*, 60, 12, (2020), 5754-5770 https://doi.org/10.1021/acs.jcim.0c00326

[22] Ruswanto Ruswanto, Richa Mardianingrum, Siswandono Siswandono, Dini Kesuma, Reverse Docking, Molecular Docking, Absorption, Distribution, and Toxicity Prediction of Artemisinin as an Anti-Diabetic Candidate, *Molekul*, 15, 2, (2020), 88-96 http://dx.doi.org/10.20884/1.jm.2020.15.2.579

[23] Christopher A. Lipinski, Lead- and drug-like compounds: the rule-of-five revolution, *Drug Discovery Today: Technologies*, 1, 4, (2004), 337-341 https://doi.org/10.1016/j.ddtec.2004.11.007

[24] Douglas E. V. Pires, Tom L. Blundell, David B. Ascher, pkCSM: Predicting Small-Molecule Pharmacokinetic and Toxicity Properties Using Graph-Based Signatures, *Journal of Medicinal Chemistry*, 58, 9, (2015), 4066-4072 https://doi.org/10.1021/acs.jmedchem.5b00104

[25] Scott A. Hollingsworth, P. Andrew Karplus, A fresh look at the Ramachandran plot and the occurrence of standard structures in proteins, *Biomolecular Concepts*, 1, 3-4, (2010), 271-283 https://doi.org/10.1515/bmc.2010.022

[26] Mohammed Zaghlool Saeed Al-Khayyat, Ammar Ghanem Ameen Al-Dabbagh, *In silico* prediction and docking of tertiary structure of LuxI, an inducer synthase of *Vibrio fischeri*, *Reports of Biochemistry Molecular Biology*, 4, 2, (2016), 66-75

[27] Atika Umi Hanif, Prima Agusti Lukis, Arif Fadlan, Pengaruh Minimisasi Energi MMFF94 dengan MarvinSketch dan Open Babel PyRx pada Penambatan Molekular Turunan Oksindola Tersubstitusi, *ALCHEMY: Journal of Chemistry*, 8, 2, (2020), 33-40 https://doi.org/10.18860/al.v8i2.10481

[28] Sedin Renadi, Anindita Tri Kusuma Pratita, Richa Mardianingrum, Ruswanto Ruswanto, The Potency of Alkaloid Derivates as Anti-Breast Cancer Candidates: In Silico Study, *Jurnal Kimia Valensi*, 9, 1, (2023), 89-108 https://doi.org/10.15408/jkv.v9i1.31481

[29] Peter W. Kenny, Hydrogen-Bond Donors in Drug Design, *Journal of Medicinal Chemistry*, 65, 21, (2022), 14261-14275 https://doi.org/10.1021/acs.jmedchem.2c01147

[30] Mohammad Sufian Badar, Shazmeen Shamsi, Jawed Ahmed, Md. Afshar Alam, Molecular Dynamics Simulations: Concept, Methods, and Applications, in: N. Rezaei (Ed.) *Transdisciplinarity*, Springer International Publishing, Cham, 2022, https://doi.org/10.1007/978-3-030-94651-7_7

[31] Xiaoxia Chen, Hao Li, Lichao Tian, Qinwei Li, Jinxiang Luo, Yongqiang Zhang, Analysis of the Physicochemical Properties of Acaricides Based on Lipinski's Rule of Five, *Journal of Computational Biology*, 27, 9, (2020), 1397-1406 https://doi.org/10.1089/cmb.2019.0323

[32] Beata Morak-Młodawska, Małgorzata Jeleń, Lipophilicity and Pharmacokinetic Properties of New Anticancer Dipyridothiazine with 1,2,3-Triazole Substituents, *Molecules*, 27, 4, (2022), 1253 https://doi.org/10.3390/molecules27041253

[33] Zakari Ya'u Ibrahim, Adamu Uzairu, Gideon Adamu Shallangwa, Stephen Eyije Abechi, Pharmacokinetic predictions and docking studies of substituted aryl amine-based triazolopyrimidine designed inhibitors of *Plasmodium falciparum* dihydroorotate dehydrogenase (PfDHODH), *Future Journal of Pharmaceutical Sciences*, 7, (2021), 133 https://doi.org/10.1186/s43094-021-00288-2